"Ersatz" and "Hybrid" NMR Spectral Estimates Using the Filter Diagonalization Method†

Clark D. Ridge and A. J. Shaka*

Chemistry Department, University of California, Irvine, California 92617-2025

Received: September 30, 2008; Revised Manuscript Received: December 31, 2008

The filter diagonalization method (FDM) is an efficient and elegant way to make a spectral estimate purely in terms of Lorentzian peaks. As NMR spectral peaks of liquids conform quite well to this model, the FDM spectral estimate can be accurate with far fewer time domain points than conventional discrete Fourier transform (DFT) processing. However, noise is not efficiently characterized by a finite number of Lorentzian peaks, or by any other analytical form, for that matter. As a result, noise can affect the FDM spectrum in different ways than it does the DFT spectrum, and the effect depends on the dimensionality of the spectrum. Regularization to suppress (or control) the influence of noise to give an "ersatz", or EFDM, spectrum is shown to sometimes miss weak features, prompting a more conservative implementation of filter diagonalization. The spectra obtained, called "hybrid" or HFDM spectra, are acquired by using regularized FDM to obtain an "infinite time" spectral estimate and then adding to it the difference between the DFT of the data and the finite time FDM estimate, over the same time interval. HFDM has a number of advantages compared to the EFDM spectra, where all features must be Lorentzian. They also show better resolution than DFT spectra. The HFDM spectrum is a reliable and robust way to try to extract more information from noisy, truncated data records and is less sensitive to the choice of regularization parameter. In multidimensional NMR of liquids, HFDM is a conservative way to handle the problems of noise, truncation, and spectral peaks that depart significantly from the model of a multidimensional Lorentzian peak.

1. Introduction

Fourier transform nuclear magnetic resonance (FT NMR) spectroscopy has efficiently and reliably delivered subtle molecular structural, stereochemical, and dynamical information in solution for decades. Two-dimensional NMR has allowed more complex spin systems to be analyzed, and multidimensional spectra with three or more frequency coordinates have expanded the applicability of NMR to larger, more complex systems.[1−3] One striking drawback of multidimensional NMR compared to one-dimensional (1D) NMR is the time needed to acquire the data in any dimension beyond the first. Obtaining data in these "indirect" dimensions requires doing a 1D NMR experiment for every point in the second dimension, a 2D experiment for every point in the third dimension, and so forth, leading to minimum experiment times of several days, or weeks, and making high-resolution, high-dimensional spectra impractical. However, in many cases, the number of expected signal peaks is constant or is only a weakly increasing function of the number of dimensions. The information content we wish to extract, measured as the number of *n*-dimensional peaks, is thus almost constant. Furthermore, the high-dimensional spectrum often allows clean separation of all peaks if the line width in each indirect dimension is narrow enough. However, indirect-dimension line widths are dominated by the transform-limited line shape, caused by the short acquisition time from the small number of time points. As a consequence, the time−frequency uncertainty principle plays a central role in the quality and clarity of the multidimensional discrete Fourier transform (DFT) spectra. Attention has thus focused on ways to gain adequate information from smaller and smaller data sets and the most information from any size data set by collecting the data differently, processing the data differently, or both. These strategies have included nonuniform sampling (NUS)[4] in tandem with maximum entropy (MaxEnt) processing,[5−7] linear prediction (LP),[8] projection reconstruction (PR),[9,10] and the filter diagonalization method (FDM).[11−16] FDM is the focus of this article.

FDM is a way to obtain a spectral estimate exclusively in terms of complex Lorentzian peaks and can deliver this estimate accurately with much shorter time signals than in the case with conventional DFT processing, as long as the data are well-matched by the model and the noise level is not too high.[15,16] An additional advantage is that, for a given signal and selection of the regularization parameter (see below), the spectral estimate is (i) unique; (ii) obtained without any assumptions or prior knowledge concerning the number or position of signal peaks; (iii) the result of a theoretically very large problem that is systematically broken down into smaller subproblems, each of which can run in parallel on a suitable digital computer, making FDM highly computationally efficient; and (iv) obtained in one step, without iteration or any danger of the problems of local minima or lack of convergence that plague nonlinear least-squares problems. That is, although the problem of fitting the multidimensional FID as a potentially very large number of complex sinusoids (each of which has an envelope that can either increase or decrease in time) appears to be a huge nonlinear least-squares problem, FDM accomplishes the task by a single linear algebra problem that has a unique solution and well-tested means to obtain it. In multidimensional spectra, a fifth point is of the utmost importance, namely, that FDM is an up-front multidimensional method that takes an *n*-dimensional time signal directly into a corresponding *n*-dimensional frequency spectrum; it is the totality of all of the data taken together that determines the achievable resolution in all of the

† Part of the "Max Wolfsberg Festschrift".

* To whom correspondence should be addressed. E-mail: ajshaka@uci.edu.

10.1021/jp808666f CCC: $40.75 © 2009 American Chemical Society
Published on Web 02/18/2009

dimensions. In multidimensional DFT spectra, each time/frequency dimension is independent; therefore, the time−frequency uncertainty principle applies to each individually. It seems that FDM uncovers correlated n-dimensional frequencies by casting the n-dimensional spectrum as a superposition of n-dimensional peaks, and nothing else.[16−20]

One limitation of FDM is that noise is not necessarily well-characterized by a collection of Lorentzian peaks or any other analytical form. In particular, n-dimensional noise distributed throughout an n-dimensional frequency space cannot be represented economically by a relatively small number of n-dimensional Lorentzian peaks. By contrast, noise responds to the DFT in a predictable manner, independent of the dimensionality of the spectrum, because the DFT is always a one-dimensional calculation in reality. The DFT of time domain noise simply shows up as frequency domain noise in the DFT spectrum. The FDM spectral estimate can have varying responses to noise, depending on the noise power and the length of the signal. One way of dealing with the noise in FDM is to use regularization to suppress the noise at the possible expense of some of the potential resolution enhancement. This regularization is especially necessary in the case of multidimensional signals.[19] Regularization broadens all peaks in the spectrum somewhat but broadens smaller peaks more. If the noise might be represented by a host of small Lorentzian peaks, regularization leads to a much smoother frequency profile, producing a spectrum with an artificial appearance. Frequency domain noise is thus not represented authentically in the regularized FDM spectral estimate. We called this synthetic, artificial spectral estimate the ersatz FDM or EFDM spectrum. Except for 1D time signals, where FDM with no regularization can be used, EFDM has been the only reasonable choice. However, the artificial noise suppression is a problem especially in two or more dimensions, where an estimated noise level is used to determine contour levels and hence what can reasonably be interpreted as a signal. As there is nothing but n-dimensional Lorentzian peaks in the FDM spectrum, it is alarmingly easy to misinterpret a noise spike as a signal. Regularization can also suppress genuine small signal peaks along with the noise, and loss of information is just what we wish to avoid. As will become clear, however, some kind of regularization appears to be essential to obtain an optimum FDM estimate, and therefore, a way to establish the true noise level is important. It is also important to reintroduce weak signal peaks that may have been regularized away.

We propose here the use of the DFT itself to reintroduce the noise, and any other missed features in the EFDM spectrum, to obtain a hybrid FDM spectrum that we denote by HFDM. Roughly speaking, we try to use FDM to represent the peaks and the DFT to represent the noise. This is done by constructing a finite-time EFDM spectrum from the parameters and subtracting it from the DFT of the measured data to give a residual spectrum. The residual contains noise, weak peaks that may have been missed, and so forth, and adding the residual to the infinite-time EFDM spectrum gives the HFDM spectrum; truncation effects have been mitigated, resolution is superior on stronger features, but all non-Lorentzian features, and the true noise, are also present. Any potential false positive feature in the infinite-time EFDM spectrum is effectively removed in the HFDM spectrum as long as it is not so narrow that it is transform-limited in the finite-time EFDM spectrum. This means that the broad, smooth description of the noise in EFDM will be subtracted out and replaced with the DFT noise in the final HFDM spectrum. Very narrow artifact peaks would appear in HFDM as a sharp spike superimposed on a transform-limited peak with opposite sign. With appropriate regularization, this does not seem to occur much.

However, it points out that the residual itself is a useful diagnostic as well. When the fit is excellent, the residual contains only noise. As the convergence of FDM depends on the local density of peaks, the quality of the fit may vary from region to region, and the residual monitors this quality. HFDM is not a new idea, having been mentioned previously,[15] but it has not been as actively explored as the more aggressive EFDM formulation, and it was introduced before the regularization method that we describe here, when it was not as crucial. The hybrid method has not been implemented in multidimensional spectra at all. Now that filter diagonalization is more mature, it is important to emphasize the most conservative and reliable implementation. In our opinion, HFDM is the choice of interest for most actual multidimensional NMR spectra.

2. Theory Section

2.1. FDM of a 1D Signal. We begin by briefly reviewing one-dimensional FDM. More complete mathematical treatments can be found elsewhere.[13,17,20] Suppose that a discrete, uniformly sampled, complex-valued, N-point time signal c_n (with N as an even number) consists of a sum of decaying sinusoidal terms

$$c_n = C(n\tau) = \sum_{k=1}^{M} d_k \exp(\mathrm{i}\{2\pi f_k + \mathrm{i}\lambda_k\}n\tau) = \sum_{k=1}^{M} d_k \exp(\mathrm{i}\tilde{\omega}_k n\tau) \qquad n = 0, \ldots, N-1 \quad (1)$$

In the practical case, the pulsed NMR FID $M_x(n\tau) + \mathrm{i}M_y(n\tau)$ would, neglecting noise, be approximated by eq 1, but for the time being, we assume that eq 1 is exact. The complex amplitudes d_k give the peak integral and relative phase, and the complex frequencies $\tilde{\omega}_k$ give the frequency position and line width over a full Nyquist spectral width $SW = \tau^{-1}$. Here, $f_k \in [-SW/2, SW/2)$ and $\lambda_k > 0$. In this case, the spectrum consists exclusively of Lorentzian peaks. The complex frequencies and amplitudes from the eq 1 can be used to compute the infinite DFT analytically. Let $u_k = \exp(\mathrm{i}\tilde{\omega}_k\tau)$, $z = \exp(2\pi\mathrm{i}f\tau)$, and $S(f)$ be the infinite DFT spectral estimate at some frequency f. Then, $S(f)$ can be computed from the parameters d_k and u_k by summing a geometric series

$$\begin{aligned} S(f) &= \frac{-\tau c_0}{2} + \tau\sum_{n=0}^{\infty}\sum_{k}^{M} d_k (u_k/z)^n = \frac{-\tau c_0}{2} + \tau\sum_{k}^{M} d_k \sum_{n=0}^{\infty} (u_k/z)^n \\ &= \frac{-\tau c_0}{2} + \tau\sum_{k}^{M} \frac{d_k}{1-(u_k/z)} = \tau\sum_{k}^{M} d_k\left(\frac{1}{1-(u_k/z)} - \frac{1}{2}\right) \end{aligned} \quad (2)$$

where the first-point correction is necessary to match the infinite DFT to the integral continuous transform, to which it should converge in the limit $\tau \to 0$. Clearly, a very fine grid can be used for the values of f, and the peaks will show no evidence of "sinc-wiggles" that are well-known artifacts in DFT spectra of truncated signals even if N is not large enough that the time $N\tau$ allows the signal to decay into the noise. Note also that eq 2 correctly takes the aliasing of the peaks by the nonzero dwell time τ correctly into account. Particularly for peaks that may be out of phase, and/or wide, it is essential to use eq 2 rather than the continuous integral formulation for the Lorentzian line shape that is often quoted in elementary texts and in some early treatments of FDM.[12,15,16]

The finite DFT for any length signal can be obtained in the same way, that is

$$S_N(f) = \frac{-\tau c_0}{2} + \tau \sum_k^M d_k \sum_{n=0}^N (u_k/z)^n$$
$$= \frac{-\tau c_0}{2} + \tau \sum_k^M \frac{d_k(1-(u_k/z)^N)}{1-(u_k/z)}$$
$$= \tau \sum_k^M d_k \left(\frac{(1-(u_k/z)^N)}{1-(u_k/z)} - \frac{1}{2} \right) \quad (3)$$

It is the second term in the numerator gives rise to the characteristic "sinc-wiggles" that appear whenever the time domain acquisition is not long enough. For decreasing exponentials, this second term becomes small once N is large enough. For increasing exponentials, however, this term can be disastrous. Equations 2 and 3 are used to form the infinite-time and finite-time EFDM spectra.

The next question is how to extract the parameters d_k and u_k from the measured data. In the conventional DFT spectrum, with no zero filling, there are N equally spaced points on a fixed frequency grid. In FDM, the number of peaks comprising the fit is $M = N/2$, that is, half of the number of data points in the FID. There are only half as many peaks because each peak requires two complex numbers to specify it, whereas one complex number specifies each of the N Fourier amplitudes. The FDM amplitudes and frequencies are obtained by an eigenvalue problem, the input matrix elements of which depend only on the discrete measured data points c_n. We assume that some "initial state" Φ_0 evolves in time and that its autocorrelation function generates the signal

$$c_n = \langle \Phi_0 | \hat{U}^n \Phi_0 \rangle \quad (4)$$

In Neuhauser's early work,[11,12] an actual autocorrelation function was the subject under study. Both $\hat{U}$ and its underlying Hamiltonian $\hat{H}$ are complex symmetric, allowing the energy states to have finite lifetimes. Here, the assumption of eq 4 is simply a convenient way to organize the problem and does not impact the scope of applicability of FDM in any way. The complex symmetric inner product, $\langle \Phi | \Psi \rangle = \langle \Psi | \Phi \rangle$ allows the initial phase of the signal to be arbitrary. (It also, however, hints at potential numerical problems as the "complex length" allows $\langle \Phi | \Phi \rangle = 0$ even for nonzero states.) Diagonalizing $\hat{U}$ and normalizing its eigenvectors is then a straightforward way to identify d_k and u_k. If we write $\hat{U}$ in its spectral representation in terms of eigenvalues and normalized eigenvectors

$$\hat{U} = \sum_k^M |Y_k\rangle u_k \langle Y_k| \quad \text{and} \quad \langle Y_k | Y_j \rangle = \delta_{kj} \quad (5)$$

then these same will exactly fit the observed time signal c_n by insertion into eq 4

$$\Rightarrow c_n = \langle \Phi_0 | (\sum_k^M |Y_k\rangle u_k \langle Y_k|)^n | \Phi_0 \rangle$$
$$= \sum_k^M \langle \Phi_0 | Y_k \rangle \langle Y_k | \Phi_0 \rangle u_k^n$$
$$= \sum_k^M \langle \Phi_0 | Y_k \rangle^2 u_k^n \equiv \sum_k^M d_k u_k^n \quad (6)$$

Note, however, that $\hat{U}$ is not known explicitly. We have only the signal points c_n as some indirect evidence of the structure of $\hat{U}$. Likewise, Φ_0 is not known explicitly. To diagonalize $\hat{U}$ numerically, a matrix representation must be obtained. This can be done by iteratively building up a basis $\{\Phi_n\}$ by translating the initial state Φ_0 in discrete time steps under the action of $\hat{U}$ to give other (nonorthogonal, unnormalized) states that can be used to make up a basis

$$\Phi_{k+1} = \hat{U} \Phi_k \quad (7)$$

Simple representations of the unit matrix, $\mathbf{1}$ or $\mathbf{U}^{(0)}$ and $\hat{U}$ or $\mathbf{U}^{(1)}$ are obtained from the measured data using this basis[13]

$$\mathbf{U}^{(0)}_{mn} = \langle \Phi_m | \Phi_n \rangle = \langle \hat{U}^m \Phi_0 | \hat{U}^n \Phi_0 \rangle = \langle \Phi_0 | \hat{U}^{n+m} \Phi_0 \rangle = c_{n+m} \quad (8)$$

$$\mathbf{U}^{(0)} = \begin{bmatrix} c_0 & c_1 & c_2 & \dots & c_{M-1} \\ c_1 & c_2 & & & \dots \\ c_2 & & & & \\ \dots & & & & \\ c_{M-1} & \dots & & & c_{2M-2} \end{bmatrix} \quad (9)$$

$$\mathbf{U}^{(1)}_{mn} = \langle \Phi_m | \hat{U} \Phi_n \rangle = \langle \hat{U}^m \Phi_0 | \hat{U}^{n+1} \Phi_0 \rangle = \langle \Phi_0 | \hat{U}^{n+m+1} \Phi_0 \rangle = c_{n+m+1} \quad (10)$$

$$\mathbf{U}^{(1)} = \begin{bmatrix} c_1 & c_2 & c_3 & \dots & c_M \\ c_2 & c_3 & & & \\ c_3 & & & & \\ \dots & & & & \\ c_M & & & & c_{2M-1} \end{bmatrix} \quad (11)$$

The eigenvalue problem

$$\hat{U} |Y_k\rangle = u_k \hat{I} |Y_k\rangle \quad (12)$$

becomes, in the new basis

$$\mathbf{U}^{(1)} \mathbf{B_k} = u_k \mathbf{U}^{(0)} \mathbf{B_k} \quad (13)$$

It is essential to include the matrix representation for the identity operator on the right-hand side of eq 13 because the basis $\{\Phi_n\}$ is not orthonormal. Likewise, the eigenvectors must be normalized with this in mind, that is

$$\mathbf{B}_k^T \mathbf{U}^{(0)} \mathbf{B}_j = \delta_{kj} \quad (14)$$

which is again somewhat different than the usual equations in quantum mechanics as the complex conjugate of the row eigenvector is not taken and $\mathbf{U}^{(0)}$ is explicitly included. Assuming eqs 13 and 14 can be solved, the FDM spectral estimate is then computed by eqs 2 and 6 as we show by explicit formulas below. Matrix diagonalization is well-understood and has been optimized extensively, making FDM efficient compared to any attempt to directly fit the FID as damped sinusoids using, for example, a nonlinear least-squares routine.[21] Nevertheless, for large experimental data sets, the $\mathbf{U}$ matrices are dense, huge, and can be ill-conditioned. These problems are partially overcome by making linear combinations of the M time-like basis functions Φ_k to form frequency-like basis functions $\Psi(f_k)$ at M equidistant frequency grid points across the spectral width, $f_k = SW[k/M - (1/2)]$, $k = 0,..., M-1$

$$\Psi(f_k) = \sum_{n=0}^{M-1} \exp(-2\pi i f_k n\tau) \Phi_n = \sum_{n=0}^{M-1} \exp(-2\pi i f_k n\tau) \hat{U}^n \Phi_0 \quad (15)$$

When we evaluate matrix elements of the $\mathbf{U}$ operators between basis functions $\Psi(f_k)$ and $\Psi(f_j)$ at widely different frequencies,

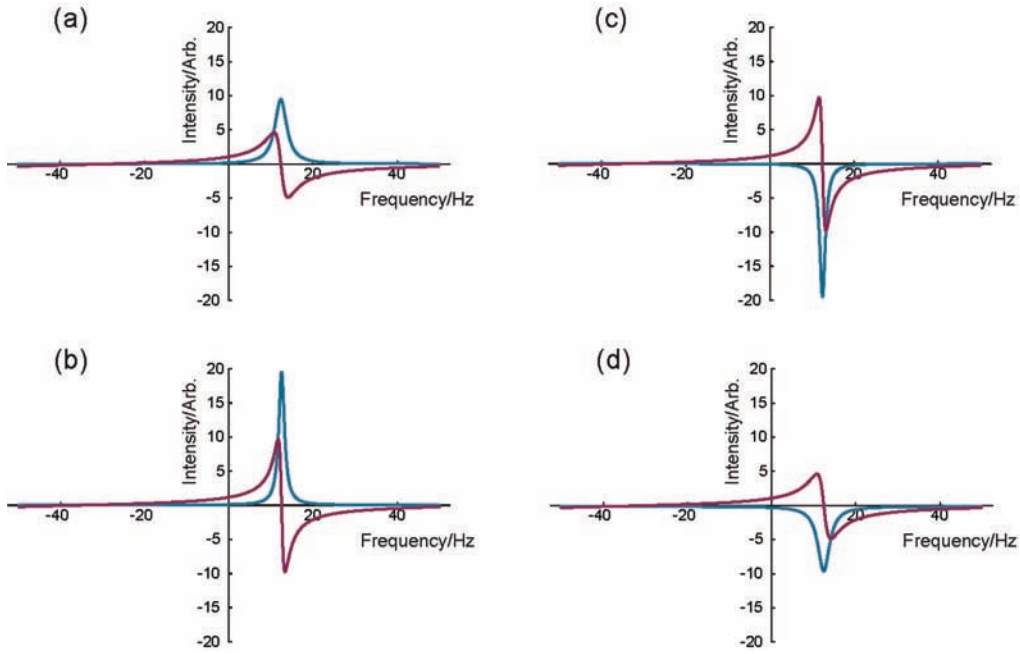

Figure 1. The behavior of a single peak with unit integral, sampled over a 100 Hz spectral width, using the analytic infinite DFT of eq 2. The real (absorption) part is shown in darkened cyan, and the imaginary (dispersion) part is shown in darkened magenta. The center of the line is at 12.5 Hz. Note that the spectrum is periodic, and the dispersion mode signal must cross through 0 as it wraps around the edges of the spectrum. (a) The eigenvalue is less than unity, $|u| = 0.90$. (b) The eigenvalue is slightly less than unity, $|u| = 0.95$. (c) The eigenvalue is slightly larger than unity, $|u| = 1.05$. (d) The eigenvalue is larger than unity, $|u| = 1.10$. While the infinite time domain signal for any eigenvalue larger than unity will diverge, the formula of eq 2 remains quite well behaved. The only pathology is that the absorption mode part changes sign.

the values are small compared to those near the diagonal—much smaller than the corresponding value between the Φ basis functions. The Fourier basis thus simplifies the structure of the matrices, making them easier to diagonalize. Small off-diagonal matrix elements, which often refer mostly to noise in any event, can safely be neglected according to time-independent perturbation theory if there is a large frequency difference between the states involved. It is this insight that allows the enormous matrix problem to yield to a divide-and-conquer strategy, in which smaller submatrices near the diagonal are solved in parallel. Physically, peaks far away from the current frequency region of interest should have very little effect on the features under study because we are tacitly assuming that the spectrum consists of "peaks" rather than delocalized features. The spectral estimate is calculated over each window by eq 2 or a number of other similar formulas[16,17] and then summed. In our current implementation of multiwindow FDM, we overlap adjacent windows by a generous 50% and use a $\cos^2$ weighting function to stitch the spectral estimates together into a full spectrum,[22] but this particular implementation is somewhat arbitrary. The idea is that the central region of the window is more accurate than the edges and therefore should be weighted accordingly. The spectra obtained are usually surprisingly insensitive to the details of the window size within broad limits. On the other hand, some peaks may be computed multiple times times, and with a different basis in each window, the results will also differ somewhat. This makes it very difficult to arrive at a line list, which is a list of each signal peak once and only once, and with the highest possible accuracy, while listing no peaks referring to noise. Thus, even though FDM is a parametric method, the output is treated not as a physical parametric description of true peaks but as a mathematical description from which the infinite DFT spectrum can be estimated.

Chopping the Fourier basis into windows provides a spectral filter that selects a certain particular spectral region for analysis (diagonalization). This rectangular Fourier filter, proposed by Mandelshtam and Taylor[13] as a refinement of Neuhauser's formulation, gives a matrix with elements that are easily computed from the signal c_n and that allows for smaller blocks of the entire matrix to be diagonalized independently. Matrix diagonalization requires numerical effort that scales as the cube of the matrix dimension; therefore, this filter diagonalization method offers a large improvement in computational time in addition to making literally any size data set susceptible to analysis. As long as the frequency width of a window is not much narrower than the true instrumental line width of a typical peak, the analysis seems to work extremely well.

Nevertheless, even in the Fourier window basis, the $\mathbf{U}$ matrices can still be quite ill-conditioned. For example, there could happen to be many more basis functions than true signal peaks or vice-versa, and the situation may vary markedly from window to window. When the matrix system is overdetermined, both $\mathbf{U}^{(0)}$ and $\mathbf{U}^{(1)}$ may become nearly singular and may in fact be exactly singular barring small amounts of noise. This is more of a problem in multidimensional FDM than in one dimension. Furthermore, noise is stationary in time, and therefore cannot possibly be properly characterized by a linear combination of only decreasing exponentials. On average, there ought to be an increasing exponential for each decreasing one. These terms have small amplitudes d_k and do not necessarily become large over the time interval for which data exist but will rapidly "blow up" if the time signal is extrapolated. Figure 1 shows this situation in a simplified way. Interestingly, while the finite DFT with a large number of points can generate a large artifact signal whenever positive exponential functions are included, the infinite DFT of eq 2 results in nothing worse than a sign change of the "peak" representing the noise. Of course, eq 2 was derived assuming that the geometric series converges, which it does not if $|u_k| > 1$. This abrupt change in the apparent sign of a peak is shown in Figure 1.

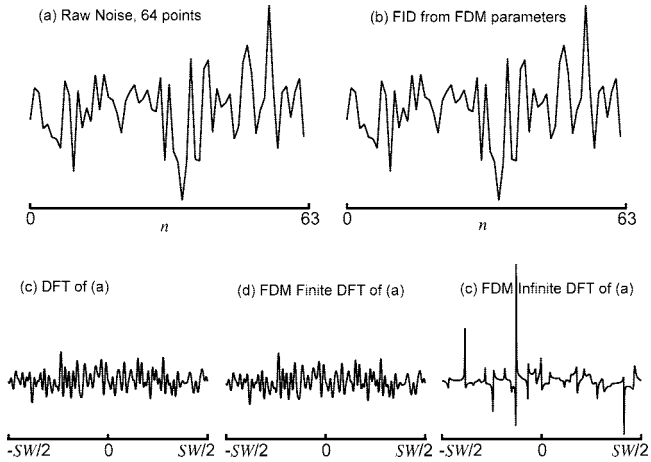

Figure 2. Demonstration of the capability to fit an arbitrary FID by the FDM parameters. In each case only the real part of the data is displayed, although all conclusions hold for both real and imaginary parts. (a) A complex 64-point FID consisting only of random noise. (b) FID resulting from the FDM parameters obtained by analyzing the data in (a) in terms of 32 complex exponentials. The fit is essentially perfect. (c) DFT spectrum of the data in (a), zero-filled to achieve a smoother interpolated appearance. (d) Finite-time analytical DFT obtained from the FDM parameters, eq 3, over the same frequency grid points as in (c). Again, the match is essentially perfect. (e) Infinite-time DFT of (a) obtained from the FDM parameters (eq 2).

2.2. Noise in FDM. The DFT can fit any time domain signal with N points sampled on a uniform time grid $n\tau$ as exactly N (nondecaying) complex sinusoids, whether the data are noise or signal. This fit is not necessarily a good spectral estimate, though, when $N\tau$ is smaller than a representative T_2. It might seem like FDM, with the flexibility to allow the frequencies to vary and the exponentials to increase or decrease, could fit the same space of functions. However, only $N/2$ such functions are allowed. It seems that in most cases of signals with N points, FDM can get an accurate fit with $N/2$ exponentials. This is shown in Figure 2. A random sequence of 64 complex numbers is fit nearly perfectly by the 32 parameters $\{d_k, u_k\}$ obtained from the generalized eigenvalue problem. However, the infinite DFT formula, eq 2, turns some of the noise peaks upside down in the spectral estimate. The finite DFT formula, eq 3, matches the finite DFT of the data but, of course, would offer no resolution enhancement for truncated signals, either. As the FDM spectral estimate may slightly mischaracterize even one-dimensional noisy data, an alternative approach is to try to avoid dealing with the noise at all, that is, trying to use FDM to fit the signals alone and then using the DFT to fit the noise. Regularization is one, albeit imperfect, way to achieve this goal.

2.3. Regularization. The primary method of addressing both the noise and the potential ill conditioning, even though these are quite separate issues, is by the use of regularization. Regularization is well-known in the context of linear least-squares problems. One has an overdetermined linear system

$$\mathbf{Ax} = \mathbf{y} \tag{16}$$

for measured (or desired) values of the vector $\mathbf{y}$ and wishes to determine $\mathbf{x}$ to solve eq 16 in the least-squares sense. When the number of equations and unknowns is identical, eq 16 can be solved by computing $\mathbf{A}^{-1}$. When the number of equations exceeds the number of unknown parameters, a singular value decomposition (SVD) of the rectangular array $\mathbf{A}$ can be used.[23] An alternative is to multiply both sides of eq 16 by $\mathbf{A}^\dagger$. This squares the condition number of $\mathbf{A}$ and is generally not good numerical practice. However, as $\mathbf{A}^\dagger\mathbf{A}$ is Hermitian and has real non-negative eigenvalues, by adding a small positive diagonal matrix (here denoted by q^2 as a reminder that is should be strictly positive), the left-hand side is assured to be nonsingular. The solution is then

$$\mathbf{x} = (\mathbf{A}^\dagger\mathbf{A} + q^2)^{-1}\mathbf{A}^\dagger\mathbf{y} \tag{17}$$

and the regularization parameter q^2 is used to control how large $|\mathbf{x}|$ is allowed to become. This well-known method goes by the names of Tikhonov regularization[24] and the moniker ridge regression in the statistics literature[25] and is commonly employed to solve ill-posed problems. With respect to the generalized eigenvalue problem, eq 13, there was apparently no similar method. Proceeding by analogy, however, we rewrote the regularized problem in the form[19]

$$\mathbf{U}^{(0)\dagger}\mathbf{U}^{(1)}\mathbf{B}_k = u_k(\mathbf{U}^{(0)\dagger}\mathbf{U}^{(0)} + q^2)\mathbf{B}_k \tag{18}$$

The effect of the regularization parameter q^2 is less obvious here. For example, we must be sure that the NMR peaks are not grossly shifted in position by including q^2. The general case of overlapping truncated peaks and noise is very complicated and probably defies any comprehensive analysis. Nevertheless, the effect of q^2 can be worked out completely for the simplest case of one sinusoid sampled at just two time points, $t = 0$ and τ.[19] There is no need to transform to the Fourier basis here, and in this case, we can write

$$c_0 = d_0 \qquad c_1 = d_0u_0 \tag{19}$$

and the generalized eigenvalue problem boils down to a 1×1 problem

$$c_1b = uc_0b \Rightarrow u = \frac{c_1}{c_0} \tag{20}$$

as long as c_0 is nonzero. Provided $|c_1| < |c_0|$, a decreasing exponential decay is predicted, and when there is no noise, $u = u_0$, as expected. However, if both c_i are small and noise is present, the uncertainty in u becomes large. Using eq 18 by contrast gives the eigenvalue

$$u = \frac{c_0^* c_1}{|c_0|^2 + q^2} = u_0\frac{|d_0|^2}{|d_0|^2 + q^2} \tag{21}$$

The second factor is real, positive, and less than unity. The frequency of the line remains unchanged, but the width increases; the line is smoothed to an extent that depends on its amplitude (d_0 is the integral of the peak not its peak intensity on resonance). If there are small features referring to noise, choosing regularization roughly similar to these amplitudes will result in a very substantial broadening of them, giving the appearance of noise suppression. Major features with amplitudes $|d_k|^2$ substantially larger than q^2 will be relatively unaffected. Regularization is thus quite different from simply applying a decreasing exponential weighting function to the FID before applying FDM as this would increase the widths of all peaks by the same amount and would not change the conditioning of $\mathbf{U}^{(0)}$ either.

There is a connection between the regularization used in FDM and that employed earlier in MaxEnt reconstruction. In MaxEnt, the idea is to find a frequency domain spectrum that is a good fit to the time domain data but not too good of a fit. That is, the fit should not be so tight that spectral features that are fitting the noise turn up. In a seminal analysis, Donoho et al.[26] rigorously showed that, in the specific case of a J-point frequency reconstruction from a J-point FID, the regularization employed in MaxEnt results in a logarithmic weighting at each

of the J frequency domain points, so that smaller points are flattened away while larger ordinates are attenuated less. In regularized FDM, it is more of a peak-by-peak weighting, achieved by a nonlinear broadening that seems to occur. A peak-by-peak weighting is somewhat more attractive because noise riding on top of peaks is not emphasized more than noise in the baseline.[27] However, it is quite obvious that neither regularized method can improve the true sensitivity of NMR spectroscopy as weak peaks are invariably discarded along with the noise and lost. Once a "peak" has been recognized above the noise, there is no real sensitivity issue whatsoever because the sensitivity is high enough to recognize the peak! It is when a signal is masked by noise that a method to retrieve it would be invaluable.

2.4. Multidimensional FDM. In two or more dimensions, several new problems arise. By analogy to eq 4, a two-dimensional time signal could be written

$$C(n_1\tau_1, n_2\tau_2) = c_{n_1 n_2} = \langle \Phi_{00} | \hat{U}_1^{n_1} \hat{U}_2^{n_2} \Phi_{00} \rangle \tag{22}$$

with two commuting operators $\hat{U}_1$ and $\hat{U}_2$. In fact, the spin Hamiltonians driving the evolution definitely need not commute. However, eq 22 is equivalent to the assumption that the 2D NMR spectrum consists solely of 2D complex Lorentzian peaks. If $\hat{U}_1$, $\hat{U}_2$ can be diagonalized simultaneously and have simultaneous eigenvectors, then

$$\begin{aligned} C(n_1\tau_1, n_2\tau_2) &= \langle \Phi_{00} | \hat{U}_1^{n_1} \hat{U}_2^{n_2} \Phi_{00} \rangle \\ &= (\Phi_{00} \{ \sum_k |Y_k\rangle u_{k1}^{n_1} u_{k2}^{n_2} \langle Y_k| \} \Phi_{00}) \\ &= \sum_k d_k u_{k1}^{n_1} u_{k2}^{n_2} \end{aligned} \tag{23}$$

and the infinite time two-dimensional DFT is then

$$\begin{aligned} S(f_1, f_2) &= \sum_k d_k (A_1(f_1) + \mathrm{i} D_1(f_1))(A_2(f_2) + \mathrm{i} D_2(f_2)) \\ &= \sum_k d_k (A_1(f_1)A_2(f_2) - D_1(f_1)D_2(f_2) + \\ &\qquad \mathrm{i}(A_1(f_1)D_2(f_2) + A_2(f_2)D_1(f_1))) \end{aligned} \tag{24}$$

where A and D are the absorption- and dispersion-mode Lorentzian line shapes and the term "phase-twist" was coined to describe the appearance of a 2D complex Lorentzian because of the way in which the apparent phase of a peak would change along adjacent traces. Note that neither the real nor the imaginary line shape is the desired double absorption line shape, A_1A_2. For this reason, most 2D NMR experiments are done in pairs, in which the modulation in F_1 can either be $\sin(2\pi i f_1 t_1)$ and $\cos(2\pi i f_1 t_1)$ or $\exp(2\pi i f_1 t_1)$ and $\exp(-2\pi i f_1 t_1)$, with the choice depending on the details of the pulse sequence. The first case is known as amplitude modulation and the second as phase modulation, with the two phase-modulated data sets being referred to as N-type (negative apparent frequency) or P-type (positive apparent frequency). Amplitude modulation is more common. A 2D complex Lorentzian phase-twist peak is well-known to have worse intrinsic resolution than the desired double-absorption line shape; therefore, sin/cos NMR data sets are always combined into a single absorption-mode spectrum during the 2D DFT.[28] However phase-modulated N- and P-type signals are the natural choice for FDM. An amplitude-modulated signal formally contains twice as many peaks as its phase-modulated counterpart, making it more likely that the number of signal peaks is larger than the basis. There are at least two possibilities: (i) combine the sine and cosine data sets into linear combinations, cos ± i sin, process each phase-modulated set separately, construct the two complex phase-twist spectral estimates, and then combine the two to obtain the absorption-mode spectrum; or (ii) simply replace the real part of the phase-twist line shape, $A_1(f_1)A_2(f_2) - D_1(f_1)D_2(f_2)$, by the double absorption line shape $A_1(f_1)A_2(f_2)$ when forming the spectrum from the eigenvalues and eigenvectors. The second possibility is the one that has been used most often for actual spectra, also using $\mathrm{Re}\{d_k\}$ as the amplitude. This presupposes that the data are correctly phased because only a single (real) spectrum is obtained.[29,30] It also may fail to give the best estimate when overlapping peaks are fit with amplitudes that have a large imaginary part. However, an advantage is that only one data set is required to obtain the spectrum. With certain popular NMR experiments employing pulsed field gradients, such as the sensitivity-enhanced HSQC experiment[31] for $^{15}\mathrm{N}-^{1}\mathrm{H}$ chemical shift correlation, it is possible to obtain a phase-modulated N-type data set without combining different transients. In this case, twice as many basis functions can be obtained if the aggressive procedure above is used.

Even if the two hypothesized evolution operators did commute, their matrix representations in a narrow-band window basis in both F_1 and F_2 would not. Moreover, when noise is included, the two matrices will not commute. This difficulty means that it is not necessarily possible to diagonalize both matrices simultaneously, obtaining a single set of eigenvectors and a pair of eigenvalues for each eigenvector. A method to try to approximately diagonalize the pair of matrices was proposed early on[32] but not followed up. Part of the difficulty is that there may not be a unique solution for "approximate diagonalization", causing possible shifts in peak positions. A more straightforward choice is to diagonalize each matrix separately and then write a formal expression for the 2D spectral estimate in terms of the eigenvalues and eigenvectors in each dimension,[32] which, using an obvious generalization of the notation of eq 2, is

$$\begin{aligned} S(f_1, f_2) = \tau_1\tau_2 \sum_{k_2}^{M} \sum_{k_1}^{M} & \langle \Phi_{00} | \mathrm{Y}_{1k_1} \rangle \langle Y_{1k_1} | \mathrm{Y}_{2k_2} \rangle \langle Y_{2k_2} | \Phi_{00} \rangle \\ & \left(\frac{1}{1 - u_{k_1}/z_1} - \frac{1}{2} \right) \left(\frac{1}{1 - u_{k_2}/z_2} - \frac{1}{2} \right) \end{aligned} \tag{25}$$

Rather than the M 2D peaks that should arise from the initial M 2D basis functions, eq 25 can generate up to M^2 peaks in a direct product pattern; in the nD case, M^n peaks may appear. If the eigenvectors are simultaneous, the cross term $\langle Y_{1k_1} | \mathrm{Y}_{2k_2} \rangle$ vanishes when $k_1 \neq k_2$, and many of these amplitudes are in fact numerically very small. Nevertheless, sensitivity to noise is amplified by the cross terms as noise affects the eigenvectors enough that spurious 2D peaks, larger than the noise floor of the 2D DFT spectrum, can arise. Regularization plays the dual role here of making the eigenvectors better behaved, so that many of the potential peaks disappear, and broadening the widths in both dimensions, so that the noise peaks are smoothed away and become less obtrusive. One danger again is that small genuine 2D peaks may be missed in the regularized spectrum. Another problem is that most NMR spectroscopists examine 2D contour plots to try to distinguish signal from noise; therefore, the unfortunate characterization of the noise as 2D Lorentzian peaks is also potentially misleading as the contoured feature can look very much like a signal. While regularization seems to be absolutely required, the very low apparent noise floor in the EFDM spectrum makes it tempting to push contour levels ever lower, making it quite possible to obtain a false positive.

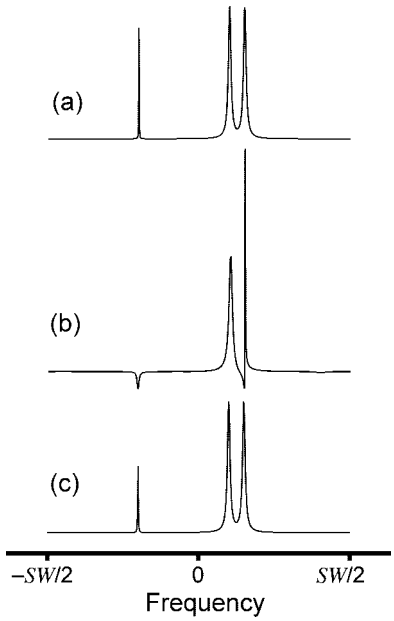

Figure 3. The effect of noise and regularization on a truncated model 1D NMR signal with three Lorentzian peaks. Only the real part of the spectrum is plotted. A doublet, each peak relative integral 1.0, and a singlet, relative integral 0.1 but with a width 10 times narrower, comprise the spectrum. (a) FDM analysis of a 16 point FID yields three peaks that match the input data exactly and 5 peaks with amplitude ~0. (b) The addition of 5% time domain noise causes errors in the eigenvalues and eigenvectors. The narrow singlet changes sign, as discussed in Figure 1. There is a noticeable error in the phase and width of the peaks comprising the doublet, as well. (c) Regularizing the generalized eigenvalue problem with eq 17 leads to a better-behaved spectral estimate. Regularization affects the width of the weakest peak more than the two stronger ones and broadens the peaks representing the noise to such an extent that they become a small DC offset that looks like a smooth background.

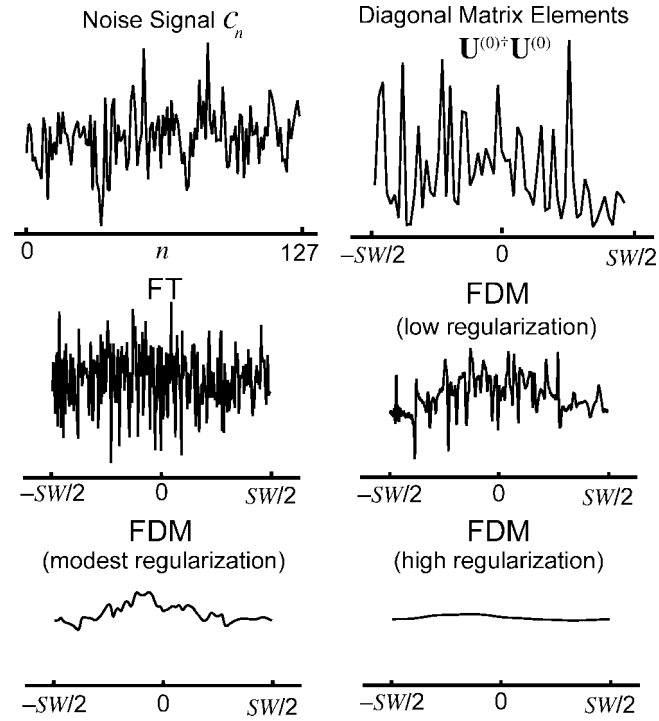

Figure 4. The successive effects of regularization on the way noise is handled by EFDM. (a) 128 points of noise, c_n, with a Gaussian distribution (the vertical scale is arbitrary). (b) The diagonal elements of $\mathbf{U}^{(0)\dagger}\mathbf{U}^{(0)}$ are plotted. They form a type of power spectrum with a strong weighting function. Their amplitude is not on the same scale as the noise time signal. (c) The DFT of the noise signal. (d−f) EFDM spectra of the noise with increasing amounts of regularization. They are regularized, respectively, with values of 1/50, 1/5, and twice the average value of the diagonal matrix elements in (b).

3. Results and Discussion

To quantify the effect of regularization on signals, noise, and artifacts in FDM spectral estimates, we examined a large number of cases by computer simulation and some data from a 2D NMR experiment. The results shown are representative of the kind of behavior to expect and are best displayed as spectra. A comprehensive analysis of the accuracy and reproducibility of peak positions and amplitudes will be pursued once the results of these Monte Carlo simulations are completed.

Figure 3 shows a simple example of the effect of a small amount of noise on a truncated model signal. There are two intense wider peaks forming a doublet and a weaker sharp singlet. The top trace is the FDM output from eqs 2, 5, 12, and 13 from a noiseless 16 point FID corresponding to just three purely Lorentzian peaks, which are obtained quantitatively. In the second trace, 5% time domain noise has been added, causing the weak narrow singlet to change sign as the imaginary park of its eigenvalue changes sign. The widths/phases of the two stronger doublets are also affected. The other five peaks, fitting the remainder of the noise, are so weak that they are hard to discern. In the third trace, the regularized EFDM spectrum is shown using eq 17 rather than eq 12. As expected, the weaker peak has selectively broadened and now has the correct phase, and the noise peaks are eliminated. It also appears that the phase and width of the doublet peaks has improved, although it is not immediately obvious why they should do so.

Figure 4 demonstrates the successive effect of regularization on a data set again consisting only of noise. The extent of regularization is best assessed by comparing it to the mean value of $\mathbf{U}^{(0)\dagger}\mathbf{U}^{(0)}$ along the diagonal. The larger the regularization, the more severe the broadening of the peaks representing the noise will be. It is not necessary in 1D FDM to broaden the noise this much. As Figure 5 shows, the regularization has the effect of shifting the eigenvalues so that they all lie within the unit circle in the complex plane. Eventually, it appears as if the noise is reduced. In actual fact, all small signals are reduced. The safest choice of regularization in 1D EFDM is that which just barely causes all of the eigenvalues to lie within the unit circle, and that value will depend on the noise level.

Figure 6shows the sequence of events that leads to the most conservative spectral estimate that FDM can offer, the HFDM spectrum. The first trace is the model data, and the next two are the DFT and nonregularized FDM results, both with added noise. FDM resolves the stronger doublet but does not do as well with the denser, weaker quartet. The next two traces show two EFDM spectra, with adequate regularization, using both the infinite DFT formula of eq 2 and the finite DFT formula of eq 3 over just the measured time interval. Due to regularization, weak peaks and/or noise will be attenuated. The finite DFT estimate should, if the fit is perfect, match the actual DFT of the data. However, the fit is not perfect because of the regularization. Taking the difference of conventional DFT and the finite DFT EFDM spectrum leaves all of the noise and/or peaks missing from the EFDM spectrum as a residual signal. If the regularization is correct and the fit is good, this signal should appear to be nothing more than noise. In the region of the doublet, the fit is apparently superior to that in the region of the quartet. Adding

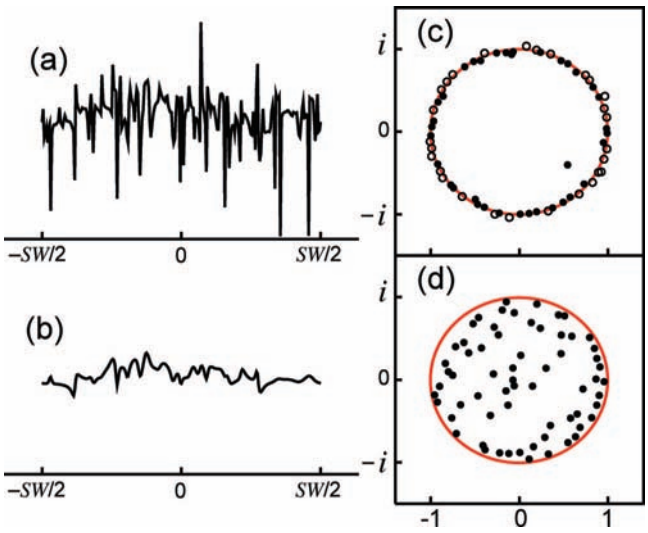

Figure 5. Spectral estimates and the position of eigenvalues u_k from the FDM calculation of pure noise. (a) The EFDM spectral estimate of unregularized noise. The noise representation shows a larger peak-to-peak amplitude than that obtained from DFT of the same data. (b) The eigenvalues returned from the unregularized generalized eigenvalue problem used to create (a). Open/filled circles show eigenvalues outside/inside of the unit circle in the complex plane. Open circles give increasing exponentials. (c) Regularization by $q^2 \sim 1/10$ of the average of the diagonal elements of $\mathbf{U}^{(0)\dagger}\mathbf{U}^{(0)}$. The noise is artificially smoothed compared to the appearance in the DFT spectrum. (d) All eigenvalues now lie inside of the unit circle.

this residual to the infinite DFT EFDM spectrum then gives the hybrid spectrum, HFDM. As Figure 6 shows, HFDM can improve the resolution of the NMR spectrum while simultaneously retaining weak peaks and correctly characterizing the noise without either artificial flattening (by the regularization) or distracting extra peaks (in the unregularized FDM estimate).

Figure 7illustrates why regularization is absolutely essential for multidimensional spectral estimation by FDM. The top panel is the unregularized FDM spectrum of a 2D HSQC spectrum of phenanthridinone (shown in the lower panel), an aromatic molecule that should show eight sets of proton multiplets with different carbon-13 frequencies. Clearly, the artifact level generated by the analytical formula of eq 25 is so high that the spectrum is of little practical value. However, a modest regularization is sufficient to attenuate these undesirable peaks. This spectrum was constructed with 2D absorption-mode Lorentzian peaks, which show a characteristic star-shaped frequency pattern, so that the only variable is the extent of the regularization. For most practical applications, a 2D Gaussian peak, giving clean elliptical contours, is preferable. It is simple to replace each Lorentzian with a Gaussian of the same integral and full width at half-height, as has been described previously.[29]

The level of regularization can easily be determined by choosing a "blank" spectral region and solving the generalized eigenvalue problem along each dimension. As the region contains only noise, the regularization should be chosen to be large enough that a flat, fairly featureless spectrum is obtained. This ensures that FDM is not attempting to fit the noise and that the direct product artifacts are not present. When there is a large level of "t_1 noise" in the interferometric dimensions, it may be necessary to increase the level of regularization somewhat so that these noisy traces are not influencing the fit much. As long as the HFDM spectrum is used, all of the noise and over-regularized features will be reintroduced by the DFT of the residual, although only within the limits of the time frequency uncertainty principle. By lowering the contour levels, the last 2D spectrum in Figure 7 demonstrates that even though noise is broadened by regularization, it is still possible to find broad peak-like features. In cases where a minor component, broadened by chemical exchange, may or may not be present, the appearance of these regularizaed noise peaks can be a distraction.

In Figure 8, traces from the 2D EFDM, DFT, and HFDM spectra are shown. The HFDM spectrum recovers some of the intensity in the weaker peak and masks the weak, broad peaks in the EFDM spectrum of Figure 7 below a sea of DFT noise.

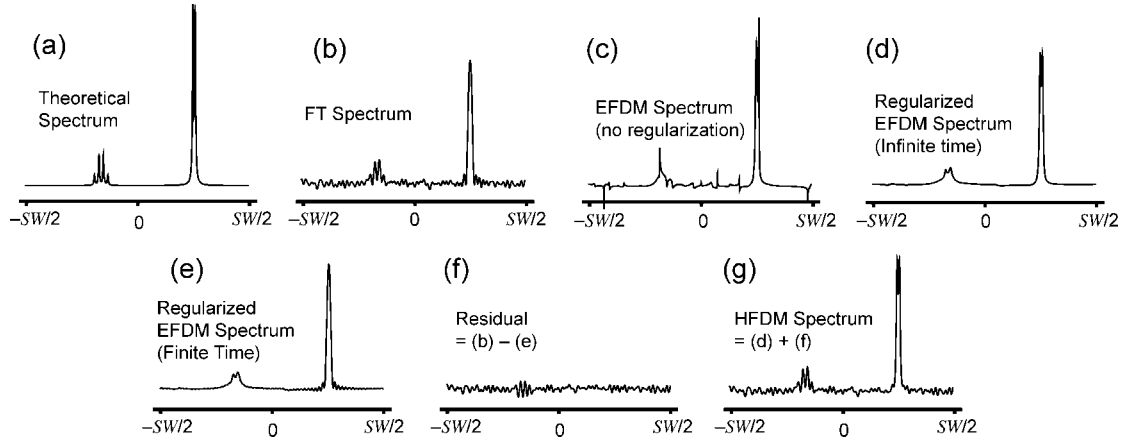

Figure 6. The combination of a regularized EFDM spectrum with the DFT of the residual signal, to give the HFDM spectral estimate. A simulated 64 point FID was used with 7.5% noise in the time domain. There are six signals, one small downfield quartet, with the outside peaks barely above the noise, and a larger upfield. (a) The model spectrum of a noise-free very long FID shows the quartet and the doublet. (b) The DFT spectrum is unable to resolve the doublet with the length of data available. (c) The FDM spectrum (no regularization) has some artifacts and distorted peaks that are introduced by the noise. (d) The EFDM spectrum, showing the noise smoothing by the regularization. The small quartet is smoothed and attenuated, however, and has an incorrect appearance. (e) The finite-time DFT estimate, eq 3, calculated with the same regularization as that in (d). (f) The residual signal, (b) − (e), which, if the fit of the signal is perfect, should consist simply of noise. In the region of the quartet, the fit is imperfect. (g) The HFDM spectrum, formed by adding the residual to the infinite-time EFDM spectrum. This spectrum captures the best of the resolving power of FDM with the unbiased noise estimate from the DFT. The doublet on the right is clearly resolved, the small quartet is resolved as well, and the noise level has also been reconstituted.

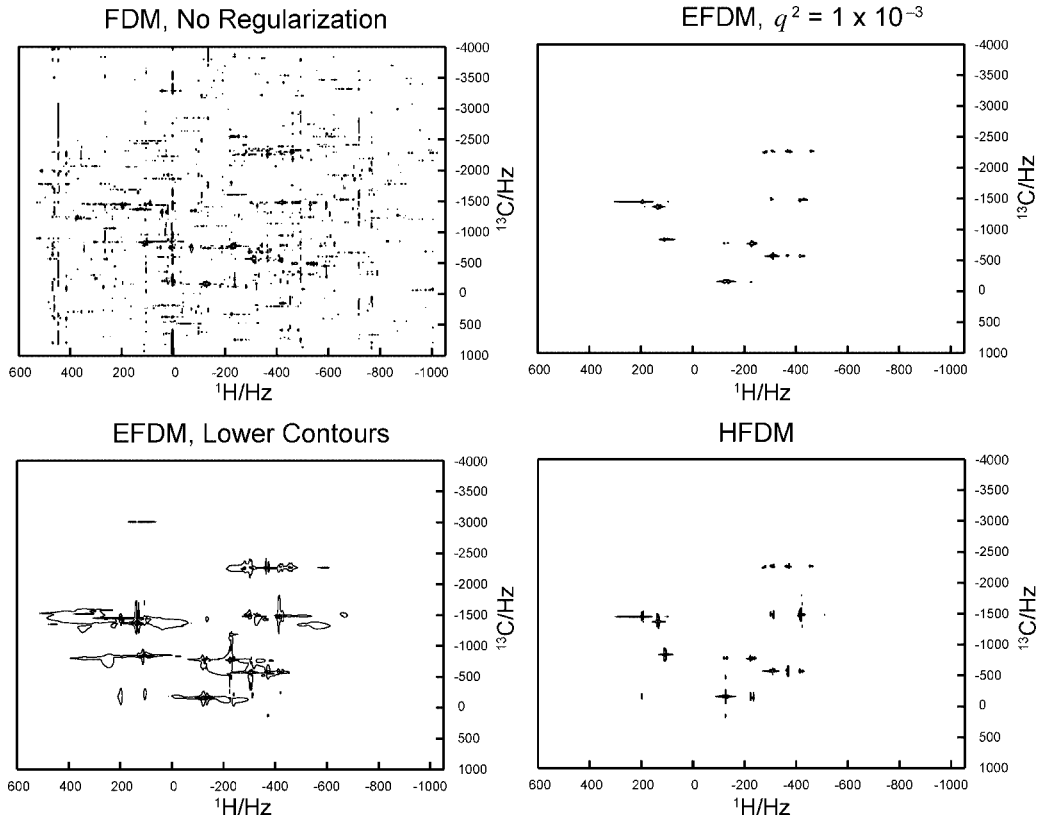

Figure 7. The dramatic effect of noise on 2D spectral estimation. The 2D $^{13}C-^{1}H$ HSQC spectrum of phenanthridinone is used as a test case. The 2D spectrum should have eight strong multiplets; no special attempt to resolve the proton−proton couplings was made, although some are resolved. (a) The 2D FDM spectrum (without regularization) obtained using eq 25. There are many, many artifact peaks for which there is no evidence in the original data. They arise because of the nonorthogonality of the two sets of eigenvectors used in eq 25. (b) The 2D EFDM spectrum using the aggressive method. The noise has been reduced, and the artifacts have been attenuated. The eight major groups of peaks for the eight directly bonded C−H pairs in the molecule show up. The regularization parameter was chosen such that a signal-free region yielded a fairly flat, featureless spectrum, indicating that the noise would probably not appear in the EFDM spectrum. Minor correlation peaks appear through a combination of long-range coupling and/or strong coupling in the ^{13}C satellite spectrum. (c) The same spectrum as that in (b) but with lower contours so that the lack of noise is apparent. Also apparent are the round peak-like features that do not resemble conventional noise, making it difficult to discern a noise feature from a small signal.

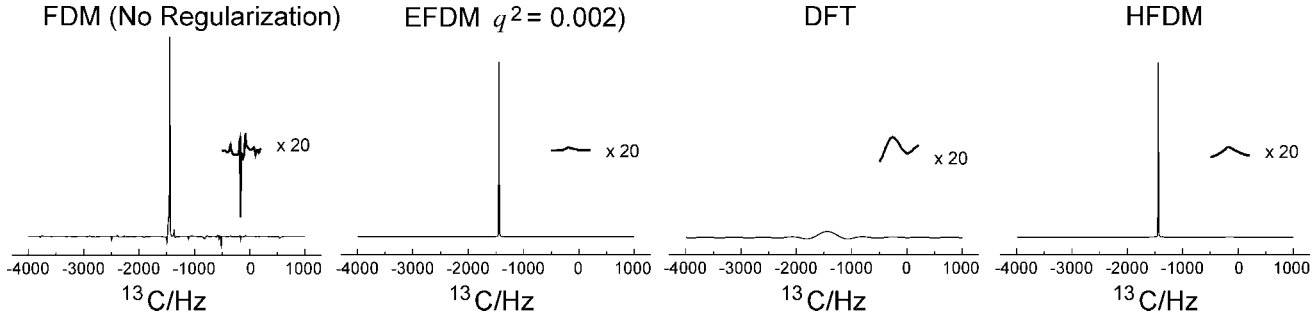

Figure 8. A set of ^{13}C traces from each of the spectra in Figure 7 (at ^{1}H, 194.6 Hz) shows the effects of regularization and the HFDM spectrum. The scale is the same for all of them, and the top of the sharp peak is not shown but is about the same size in all three. There is a small feature on the left that is below the level of the artifacts in the first spectrum and is attenuated severely in the second, regularized trace. The third trace shows the peak restored above the low level of the noise.

At high enough contour levels, the EFDM and HFDM contour plots are quite similar.

4. Conclusions

The hybrid, or HFDM, spectrum is a conservative approach to handle noisy, truncated NMR data in a numerically stable and efficient way. Conceptually, HFDM uses filter diagonalization to pick out signal peaks that are both strong enough to rise above the noise and close enough to the Lorentzian model to be a decent fit. The noise is then characterized by the more familiar DFT by adding a residual signal to the synthetic, relatively noise-free EFDM spectrum. Noise, although it can certainly be accurately fit in the time domain for 1D NMR signals, gives an unfamiliar frequency domain representation in terms of Lorentzian peaks, and in the infinite DFT estimate, some noise peaks or narrow weak signal peaks may invert. Particularly in two dimensions (or higher), where noise has the more pernicious effect of generating a host of direct product artifact peaks, it is essential to regularize the generalized eigenvalue problem. This regularization will tend

to broaden all peaks, but smaller peaks and noise will be most affected. Reestablishing the true noise level and recovering any weak peaks then lead to the HFDM spectral estimate.

Regularization, if only the ersatz, or EFDM, spectrum will be used, should be sparingly applied as weak signal peaks may well be lost. However, by instead using the HFDM spectrum, the result is somewhat less sensitive to the level of regularization. Indeed, if the regularization is very severe, so that even major peaks are broadened excessively, the HFDM spectrum simply reverts to the conventional DFT spectrum, making it a no-lose proposition for the conservative analysis of NMR data. In 3D and 4D NMR, the same principles apply, and the noise level is even more important to avoid false positive peaks that can occur by contouring planes out of the high-dimensional data. In addition, the residual spectrum provides an important clue concerning the accuracy of both the Lorentzian model, the FDM way of obtaining the fit, and the amount of data available. Further applications of these aspects of HFDM are under active development and will be described in future publications.

Acknowledgment. This material is based upon work supported by the National Science Foundation under CHE-0703182. The authors are indebted to Prof. V. A. Mandelshtam for helpful discussion and insight.

References and Notes

(1) Scott, L. G.; Hennig, M. *Methods Mol. Biol.* **2008**, *452*, 29–61.
(2) Foster, M. P; McElroy, C. A.; Amero, C. D. *Biochemistry* **2007**, *46*, 331–340.
(3) Mittermaier, A.; Kay, L. E. *Science* **2006**, *312*, 224–228.
(4) Hoch, J. C.; Maciejewski, M. W.; Filipovic, B. *J. Magn. Reson.* **2008**, *193*, 317–320.
(5) Gull, S. F. *Nature* **1978**, *272*, 686–690.
(6) Skilling, J. *Nature* **1984**, *309*, 748–749.
(7) Hore, P. J. *J. Magn. Reson.* **1985**, *62*, 561–567.
(8) Stephenson, D. S. *Prog. Nucl. Magn. Reson. Spectrosc.* **1988**, *20*, 515–626.
(9) Kupce, E.; Freeman, R. *J. Am. Chem. Soc.* **2003**, *125*, 13958–13959.
(10) Crowther, R. A.; Derosier, D. J.; Klug, A. *Proc. R. Soc. London, Ser. A* **1970**, *317*, 319–340.
(11) Neuhauser, D. *J. Chem. Phys.* **1994**, *100*, 5076–5079.
(12) Wall, M. R.; Neuhauser, D. *J. Chem. Phys.* **1995**, *102*, 8011–8022.
(13) Mandelshtam, V. A.; Taylor, H. S. *J. Chem. Phys.* **1997**, *107*, 6756–6769.
(14) Mandelshtam, V. A.; Taylor, H. S. *J. Chem. Phys.* **1998**, *108*, 9970–9977.
(15) Mandelshtam, V. A.; Taylor, H. S.; Shaka, A. J. *J. Magn. Reson.* **1998**, *133*, 304–312.
(16) Hu, H.; Van, Q. N.; Mandelshtam, V. A.; Shaka, A. J. *J. Magn. Reson.* **1998**, *134*, 76–87.
(17) Mandelshtam, V. A. *J. Magn. Reson.* **2000**, *144*, 343–356.
(18) Hu, H.; De Angelis, A. A.; Mandelshtam, V. A.; Shaka, A. J. *J. Magn. Reson.* **2000**, *144*, 357–366.
(19) Chen, J. H.; Mandelshtam, V. A.; Shaka, A. J. *J. Magn. Reson.* **2000**, *146*, 363–368.
(20) Mandelshtam, V. A. *Prog. Nucl. Magn. Reson. Spectrosc.* **2001**, *38*, 159–196.
(21) Gesmar, H.; Led, J. J.; Abildgaard, F. *Prog. Nucl. Magn. Reson. Spectrosc.* **1990**, *22*, 255–288.
(22) Chen, J. H.; De Angelis, A. A.; Mandelshtam, V. A.; Shaka, A. J. *J. Magn. Reson.* **2003**, *162*, 74–89.
(23) Golub, G. H.; Reisch, C. *Numer. Math.* **1970**, *14*, 403–420.
(24) Tikhonov, A. N. *Sov. Math. Dokl.* **1963**, *4*, 1035–1038.
(25) Marquardt, D. W. *Technometrics* **1970**, *12*, 591–612.
(26) Donoho, D. L.; Johnstone, I. M.; Stern, A. S.; Hoch, J. C. *Proc. Natl. Acad. Sci. U.S.A.* **1990**, *87*, 5066–5068.
(27) Hoch, J. C.; Stern, A. S. *NMR Data Processing*; Wiley−Liss: New York, 1996; Chapter 4.
(28) States, D. J.; Haberkorn, R. A.; Ruben, D. J. *J. Magn. Reson.* **1982**, *48*, 630–632.
(29) Chen, J.; De Angelis, A. A.; Mandelshtam, V. A.; Shaka, A. J. *J. Magn. Reson.* **2003**, *162*, 74–89.
(30) Armstrong, G. A.; Cano, K. E.; Mandelshtam, V. A.; Shaka, A. J.; Bendiak, B. *J. Magn. Reson.* **2004**, *170*, 156–163.
(31) Muhandiram, D. R.; Kay, L. E. *J. Magn. Reson.* **1994**, *103*, 203–216.
(32) Wall, M. R.; Dieckmann, T.; Feigon, J.; Neuhauser, D. *Chem. Phys. Lett.* **1998**, *291*, 465–470.

JP808666F